

Anatomy, modelling and prediction of aeroservoelastic rotorcraft-pilot-coupling.

M. Gennaretti, M.M. Collela, J. Serafini, B. Dang Vu, P. Masarati, Giuseppe Quaranta, V. Muscarello, M. Jump, M. Jones, L. Lu, et al.

▶ **To cite this version:**

M. Gennaretti, M.M. Collela, J. Serafini, B. Dang Vu, P. Masarati, et al.. Anatomy, modelling and prediction of aeroservoelastic rotorcraft-pilot-coupling.. 39th European Rotorcraft Forum, Sep 2013, MOSCOU, Russia. hal-01061273

HAL Id: hal-01061273
https://onera.hal.science/hal-01061273

Submitted on 5 Sep 2014

HAL is a multi-disciplinary open access archive for the deposit and dissemination of scientific research documents, whether they are published or not. The documents may come from teaching and research institutions in France or abroad, or from public or private research centers.

L'archive ouverte pluridisciplinaire **HAL**, est destinée au dépôt et à la diffusion de documents scientifiques de niveau recherche, publiés ou non, émanant des établissements d'enseignement et de recherche français ou étrangers, des laboratoires publics ou privés.

ANATOMY, MODELLING AND PREDICTION OF AEROSERVOELASTIC ROTORCRAFT-PILOT-COUPLING

Massimo Gennaretti, Marco Molica Colella, Jacopo Serafini
University Roma Tre, Dept. of Engineering, Rome, Italy - m.gennaretti@uniroma3.it

Binh Dang Vu
ONERA, Salon de Provence, France

Pierangelo Masarati, Giuseppe Quaranta, Vincenzo Muscarello
Politecnico di Milano, Dept. of Aerospace Engineering, Milano, Italy

Michael Jump, Michael Jones, Linghai Lu
University of Liverpool, School of Engineering, Liverpool, United Kingdom

Achim Ionita, Ion Fuiorea, Mihai Mihaila-Andres, Radu Stefan
STRAERO, Bucharest, Romania

Abstract

Research activity and results obtained within the European project ARISTOTEL (2010-2013) are presented. It deals with anatomy, modelling and prediction of Rotorcraft Pilot Coupling (RPC) phenomena, which are a really broad and wide category of events, ranging from discomfort to catastrophic crash. The main topics concerning piloted helicopter simulation that are of interest for designers are examined. These include comprehensive rotorcraft modelling suited for Pilot Assisted Oscillations (PAO) prediction, modelling of pilot biodynamics behaviour in the PAO frequency range of interest, definition and application of criteria for detection of RPC instabilities of aeroservoelastic nature. The numerical investigation considers Bo105 and IAR330 Puma helicopter models, as representatives of two different rotorcraft categories (small-size and medium-size helicopters, respectively). Factors affecting aeroservoelastic RPC prediction are investigated (like, for instance, pilot modelling, system modelling, number of controls on which the pilot exerts forces, control chain gearing ratios), with the aim of defining design guidelines for prevention of adverse RPCs occurrence.

1. INTRODUCTION

The term 'Aircraft/Rotorcraft Pilot Coupling' (A/RPC) relates to an extremely wide category of events. Despite the final effects of A/RPCs being similar, ranging from mild pilot discomfort to a catastrophic crash, the underlying causes can be very different. Over the last few years, the rotorcraft scientific community has focused its attention on these very complex events, following the lead of earlier research efforts undertaken by the fixed-wing aircraft community. A detailed review of the mechanisms that lead to A/RPC phenom-

ena as well as the research activity already performed in this field are given in Ref. [1]. As part of this renewed research effort, the ARISTOTEL project aims to develop tools and techniques to predict the susceptibility of modern fixed- and rotary-wing aircraft to A/RPC, and to develop guidelines to allow the design of next the generation of these aircraft such that adverse A/RPCs can be avoided. This paper reports on the activity and results obtained within the European project ARISTOTEL (2010-2013) and specifically on the anatomy, modelling and prediction of aeroservoelastic Rotorcraft Pilot Coupling phenomena [2].

In the past, it has often been very difficult to recognize and then analyse an RPC event. This is partly due not only to the challenge of reconstructing what happened from an accident scene, but also because of the lack of awareness of these events on the part of possible witnesses, even when they are highly trained individuals. Indeed, RPC events are always associated with a mismatch between the pilot's mental model of the vehicle's dynamics and actual motion taking place. This is true even as a catastrophic event unfolds. The analysis of these events is very complex as it involves rigid body dynamics, aeroservoelasticity, the automatic flight control system and, of course, biodynamics and piloting [1]. In the preceding years, an effort has made by the research community to distinguish between RPC events by introducing different classes. The most functional classification is based on the frequency content of the dynamics involved, for which Rigid Body RPCs (frequency range $0-2$ Hz) are separated from Aeroelastic RPCs (frequency range $2-8$ Hz). In the first class of phenomena, sometimes known as Pilot Induced Oscillations (PIOs), the pilot response is dominated by a behavioural process (a mental mismatch, as stated above), whereas in the latter, known as Pilot Assisted Oscillation (PAO), the pilot becomes as an unconscious link between the seat motion and the controls, thus acting like a mechanical impedance [1]. In contrast to the fixed-wing world, where most APC events are characterized as PIOs, the available records clearly show that PAOs contribute to a significant proportion of RPC accidents and thus requiring greater attention in by the rotary-wing community [3]. For the frequency range involved in PAOs, the pilot's unintentional control input actions couple with, for example, rotor blade dynamics, airframe flexibility and servos, amongst others, thus requiring more complex tools for effective computational simulations. Moreover, due to their low frequency nature, some aeroelastic phenomena may play a non-negligible role in helicopters PIOs [1, 4].

The aeroservoelastic phenomena-related ARISTOTEL project activities have focussed on the main topics concerning piloted helicopter simulation that are of interest for designers. These range from comprehensive rotorcraft modelling suited to PAO phenomena prediction, modelling of pilot biodynamic behaviour in the PAO frequency range of interest and the definition and application of criteria for detection of RPC instabilities of an aeroservoelastic nature. The workload has been shared amongst the partners as follows:

- ONERA has undertaken helicopter modelling and analysis using the state-space formulation available in the HOST tool [5], concentrating on the frequency region of interest where rigid-body and aeroelastic RPCs overlap;
- Politecnico di Milano (PoliMi) have investigated helicopter-pilot interaction modelling using two approaches: one using a state-space tool, MASST [6], that blends together a collection of sub-models from well-known, reliable and possibly state-of-the-art sources; the second derives helicopter dynamics within the MultiBody tool MBDyn which is capable of performing non-linear analysis based on first principle solutions (http://www.mbdyn.org/);
- STRAERO focused their attention on the detection of instabilities and limit cycles from high fidelity aeroelasticity modelling, as well as on power spectral density analysis of linearised helicopter models with additional rate-limits elements to assess their effect on handling qualities;
- University of Liverpool (UoL) activity was dedicated to the development of linear and non-linear helicopter models for real-time simulations conducted in the HELIFLIGHT simulator;
- University Roma Tre (UROMA3) dealt with the development of helicopter models with different levels of fidelity (particularly in the aerodynamic components), performing both eigenvalue and non-linear time-marching solutions for analysis and detection of instabilities.

As already stated, these research activities aim at the definition of modelling requirements and validated computational tools for pilot-in-the-loop analyses, with the final goals of (i) identification of potential sources/critical parameters for adverse aeroservoelastic RPCs, and (ii) definition of design guidelines and methodologies for the prevention of adverse RPC/PAO in the future helicopter generation.

The first part of the paper is dedicated to the description of ARISTOTEL partners helicopter models and the issues encountered. The second part of the paper is focused on pilot-in-the-loop analyses. A number of factors affecting the prediction of aeroservoelastic RPCs are investigated, including pilot modelling, the number of controls on which the pilot exerts a force, control chain gearing ratios and flight conditions. The numerical investigation concerns a small helicopter (Bo-105) and a medium helicopter (IAR330 Puma). These vehicles were chosen not only as being representative of the two different rotorcraft categories but also because of the availability of data for each of them. Results derived from the different approaches applied by the ARISTOTEL partners for PAO instability detection (ranging from eigenvalue to non-linear time-marching analyses, as mentioned above) are presented and discussed.

2. METHODS OF ANALYSIS

In the following Section, the analysis methodologies used by the ARISTOTEL partners to investigate aeroservoelastic RPC phenomena are briefly outlined. Although each Section relates to a single partner, the activities developed on a collaborative basis are also described. These represent a point of strength of the project ARISTOTEL.

2.1 ONERA

ONERA has conducted analytical investigations in the area of linear and non-linear RPC by extending the analysis performed for rigid-body models [7] to the frequency region where rigid-body and aeroelastic RPCs overlap. The research is oriented toward developing aeroelastic models and applying existing RPC prediction criteria and stability analysis tools. ONERA has developed non-linear models of the IAR330 Puma helicopter in the HOST [5] simulation environment using the rotorcraft database available in ARISTOTEL. The model has a rigid fuselage and an elastic main rotor. Linearized models of order 26 around the hover flight condition and of order 62 around forward flight conditions have been derived for the application of RPC prediction tools. A flight control system (FCS) with rate command-attitude hold (RCAH) flight control laws has been developed to improve the handling qualities of the bare airframe helicopter while leaving the rotor elastic modes unchanged.

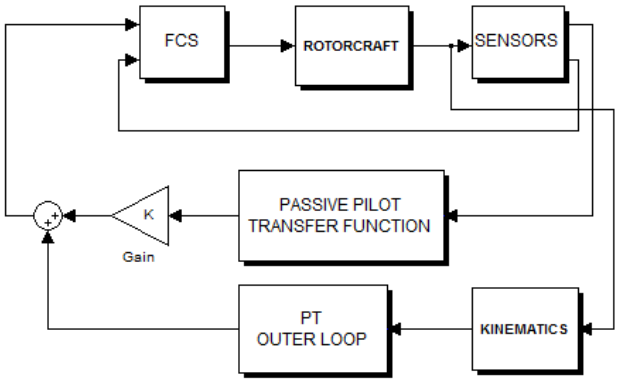


Figure 1. Coupled pilot-vehicle system.

The analysis proceeds as follows. First, the RPC analysis is performed with the bandwidth-phase delay prediction criterion. Bandwidth-phase delay has been shown to be an effective criterion to discriminate Category I PIO tendencies for rigid-body helicopters [7].

Second, the passive coupling of the pilot biomechanics with the aeroelasticity of the rotorcraft is analysed using a classical eigenvalues method. Figure 1 presents the coupling scheme of the pilot-vehicle system with the passive pilot closing the loop through the gain K.

Third, the behaviour of the vehicle coupled with a combined passive/active pilot in the loop is predicted by using an eigenvalues analysis method. The piloting task is a point tracking (PT) task, consisting of a roll-step manoeuvre followed by the stabilization of the ground track of the helicopter trajectory inside boundaries indicated by markers aligned on the ground.

The application of the bandwidth-phase delay PIO criterion does not require a pilot model. The passive pilot model used in the eigenvalues analysis study is rep-

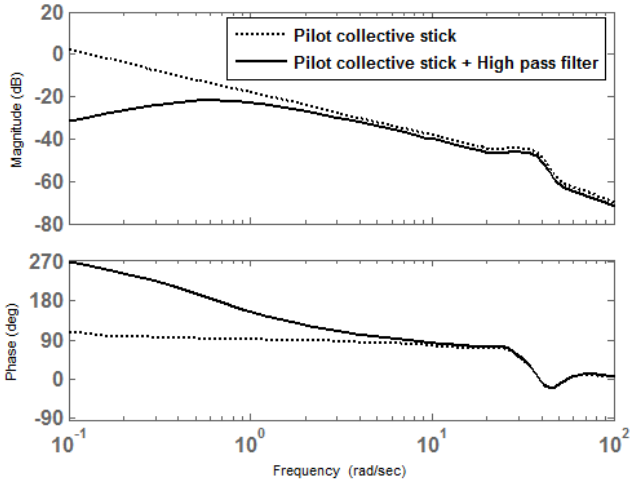


Figure 2. Relative collective control rotation transfer function.

resented by transfer functions using pilot seat accelerations as input and control inceptor (collective and cyclic) accelerations normal to the handle as output. The transfer functions have been identified by PoliMi from experiments conducted in UoLs HELIFLIGHT simulator [8]. For example, Figure 2 shows the Bode diagram of the relative collective control rotation transfer function which is characterised by poles at $-68.46 \pm 23.35i$, $-6.85 \pm 38.28i$, $-5.08 \pm 24.44i$, and 2 poles at the origin. The low-frequency behaviour of the pilot transfer function is corrected by adding a washout high-pass filter.

The point tracking task is formulated as a common guidance and control problem separating an outer guidance loop and an inner control loop. The inner control loop consists of the full-authority RCAH control law mentioned above. The outer loop model assumes that the pilot first processes raw perceptual input by a Kalman filter which yields estimates of the vehicle and disturbance states. This model also assumes that the pilot has internal models of the vehicle dynamics and the disturbance inputs that can be represented mathematically in a common, earth-fixed inertial frame of reference. The model also assumes that the pilot operates upon these estimates using an optimal controller. Typically, proportional and derivative controllers are used on the cross-track error. For the roll step manoeuvre, pitch, roll and yaw rates commands are thus generated in order to perform the bank angle required to nullify the cross-track error.

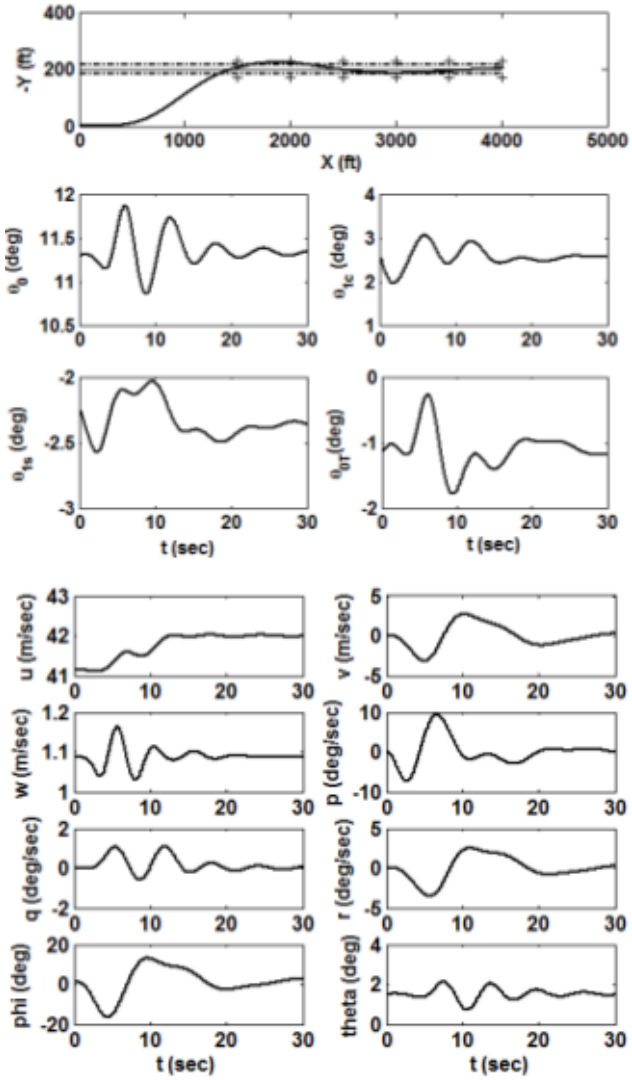


Figure 3. IAR330 Puma roll step manoeuvre.

The time histories of the active pilot model performing a roll step manoeuvre with the aeroelastic IAR330 model are shown in Figure 3 (where: u, v, w denote body-axes, airspeed components; p, q, r denote body-axes, roll, pitch, yaw rates; ϕ, θ denote roll and pitch angles; $\theta_0, \theta_{1c}, \theta_{1s}, \theta_{0T}$ denote collective, lateral cyclic, longitudinal cyclic and collective tail rotor commands from control actuator). The adequate performance is represented by the cross markers and the desired performance is represented by the dash-dot lines. The desired performance requirements are met through coordinated actions of the controls: speed deviation 5 kts, lateral deviation at markers 15 ft, heading 10 deg, roll attitude at markers 5 deg, height 10 ft.

2.2 Politecnico di Milano

In order to investigate PAO events, Politecnico di Milano has developed linear and non-linear aero-servo-elastic models of the IAR330 Puma and of the Bo105 in MASST and MBDyn.

Linear bio-aeroservoelastic stability analyses have been performed on the the Bo-105. It has been found that unstable lateral oscillations appear when considering the pilot/lateral stick model in the feedback loop with the rotorcraft dynamics. PAO instabilities have been predicted using three pilot/lateral stick transfer functions identified during the experimental test campaign performed at UoL in July 2012 [10]. Stability analyses were performed using the Nyquist criterion for SISO systems, considering the feedback loop between the lateral acceleration at the pilot seat, a_y, and the lateral displacement of the stick, δ_y. The SISO transfer function of the Bo-105 helicopter at 80 kts, $a_y = H(s) \cdot \delta_y$, has been obtained using MASST. The investigated Loop Transfer Function (LTF) of the Pilot Vehicle System (PVS) model is

$$\text{LTF}(s) = -G_y \cdot \exp(-\tau_y \cdot s) \cdot H(s) \cdot H_{\text{PP}}(s)$$

where G_y and τ_y are respectively the gain and the time delay on the lateral cyclic control and $H_{\text{PP}}(s)$ is the identified pilot/lateral stick transfer function. The analyses have been parametrized at different gains G_y and time delays τ_y, considering the three test pilot's biodynamics in the feedback loop with the aeroservoelastic model of the Bo105 at 80kts.



Figure 4. Test subject inside the flight simulator grasping the collective lever (left) and multibody model of the pilot's arm (right).

Vertical bounce predictions have been performed with the multibody model of the IAR330 Puma [11], coupled with the detailed biomechanical model of the pilot's arm proposed in Ref. [12]. In the following, the detailed multibody model of the pilot's arm, shown in Fig. 4, is directly coupled to the multibody model of the helicopter to assess the feasibility of integrated bio-aeroservoelastic simulations. The essential changes consist of connecting both the shoulder attachment point and the hinge of the collective control device to the finite element model of the helicopter's airframe, and of passing the collective control rotation as an input to the flight control system. The rotation of the control device about its hinge is scaled using the gearing ratio on the collective lever to produce the desired command to the swashplate actuators. Results have been obtained while performing the vertical manoeuvre defined in the Helicopter Aeronautical Standard Design 33 (ADS-33, Ref. [9]), using different gearing ratios in the collective control loop.

2.3 University of Liverpool

As part of the activities for ARISTOTEL, UoL has implemented aeroelastic models in FLIGHTLAB [15] within the simulation facility to provide a real-time aeroelastic simulated flight test capability to the project. Three different models have been developed:

- a simple 2-degree-of-freedom (2DOF) aeroelastic heave and lateral model provided by PoliMi;
- two 74th-order linear models based on the Bo105 and IAR330 Puma rotorcraft (the models are in a state-space form, the state matrices having been obtained using MASST [6] from PoliMi);
- two non-linear multi-body aeroelastic FLIGHTLAB helicopter models based upon the Bo105 and IAR330 Puma airframes which incorporate elastic rotor and fuselage models.

These models have served as the test beds for the investigations into aeroelastic RPC phenomena. The linear models have already been used for a PAO test campaign [16]. This paper reports results on the development of the aeroelastic Bo105 and IAR330 Puma helicopter models in the real-time simulation environment. Due to their additional complexity, they are perhaps more representative of an industry-relevant model development process. The development process of the

aeroelastic Bo105 and IAR330 Puma models in FLIGHTLAB can be divided into two phases: the development of an isolated elastic rotor model and then the development of elastic fuselage model. This first phase uses specific utilities/methods that are available in FLIGHTLAB and is the first step to building a multi-body dynamics model that incorporates aeroelastic effects.

2.4 STRAERO

2.4.1 Advanced rotorcraft model for aeroelastic RPC analysis

Part of the activity undertaken by STRAERO within the ARISTOTEL project has focused on high fidelity aeroelastic simulations of the IAR330 Puma rotorcraft.

The blade structure has been simulated through a FEM model, validated against modal and gravimetric tests [18]. The fluid domain was chosen as a continuous air ideal gas, discretized by a deformable mesh. The Navier-Stokes equations to be solved were closed with a shear stress transport with automatic wall function model of turbulence, and the boundary layer was solved with the scalable wall function model. Scalable wall functions overcome one of the major drawbacks of the standard wall function approach, in that they can be applied on arbitrarily fine meshes. For rotorcraft blades, the wall, moving surface, boundary condition type was adopted, so as to apply the mesh displacement predicted by the structural solver [19]. In order to preserve the displacements received from the structural solver, these have been interpolated using the profile preserving method.

Since there is a strong coupling between the rotorcraft structure and the flow field, STRAERO used a two way fluid-structure interaction analysis to predict blade loads and vortex shedding in the hover condition. The numerical solution algorithm is based on the basic staggered solution for the partitioned analysis of coupled equations described in Ref. [20]. Coupled simulations follow a time-step/iteration scheme: the fluid solver and the structural solver execute the simulation through a sequence of multi-field time steps, each of which consists of one or more ”stagger” (or coupling) iterations. At every stagger iteration, each field solver gathers the data it requires from the other solver and solves its field equations for the current multi-field time step. This process is repeated until a maximum number of iterations is reached or until the transferred data have converged.

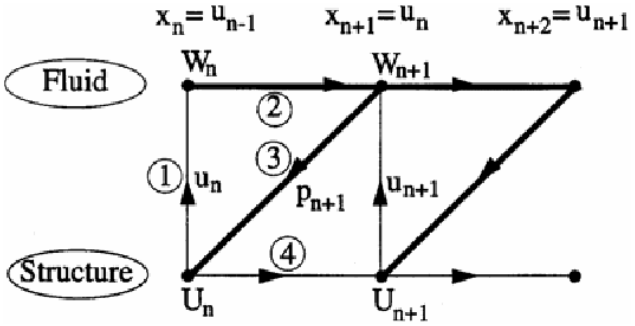


Figure 5. Basic staggered algorithm [20].

2.4.2 Rotorcraft susceptibility to RPC

The GARTEUR AG-15 and GARTEUR HC-16 action groups were dedicated to research into adverse vehicle-pilot couplings (A/RPC). A refined method for Pilot-in-the-Loop analysis in the programs described above has been the Power Spectral Density (PSD) method to predict the vehicle handling qualities level based on the revised structural model of the human operator developed by R. Hess [21]. The key element in this method is the evaluation of the pilots control activity in different mission tasks. The metric used to determine PIO susceptibility is the power spectral density of the proprioceptive feedback signal. A pilot-vehicle PSD analysis has been conducted using the vehicle configurations from the PoliMi database for the IAR330 Puma linearized dynamics [22]. This can provide the prediction of the vehicle's handling qualities level in a single axes task with linear or non-linear dynamics. The study of category I and II RPC/PIO susceptibility has been developed by the selection of different configurations of linearized rotorcraft dynamics with additional displacement limit elements in the servo-actuators of the control chains.

Figure 6 shows a block diagram representation of the aero-servo-elastic model built by PoliMi. Their dynamics include 6 rigid body modes, 8 structural fuselage modes and 14 main-rotor aero-elastic modes with additional axial dynamic inflow states. The rotorcraft dynamics are completed by 4 servo-actuators on the main controls and 4 controllers dynamics to improve stability performance. In addition, this scheme also included

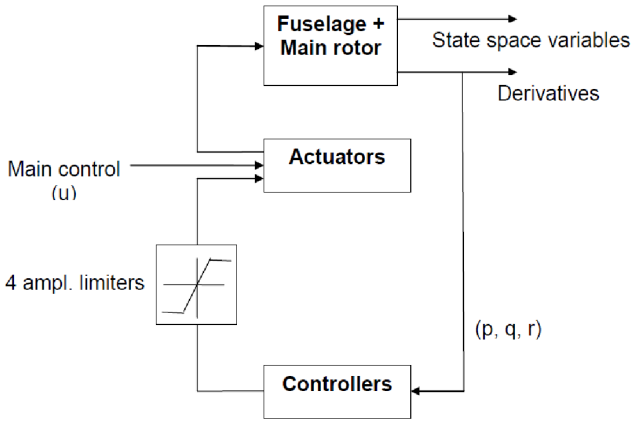


Figure 6. Modified aeroservoelastic PUMA model with displacement limiters.

the amplitude limits for the collective, longitudinal and lateral cyclic and tail rotor actuators.

The handling qualities sensitivity function (HQSF), removing the effects of control sensitivity, is defined as

$$\text{HQSF} = M(j\omega)/C(j\omega)(1/K_e)Y_{PF}(j\omega)/Y_c(j\omega)$$

where Y_c denotes the transfer function of vehicle dynamics, M is the output of the structural pilot model (SPM), C is the input to the SPM, Y_{PF} denotes the transfer function of the proprioceptive feedback element in SPM, whereas K_e is the error gain in SPM. The RPC/PIO assessment technique utilizes the power spectral density (PSD) of a signal, u_m, as in Ref. [21] with the control sensitivity removed, considering the normalized PSD of the input given by

$$\Phi_{u_m u_m}(\omega) = 2^4 \left|\text{HQSF}\right|^2/(\omega^4 + 2^2)$$

As suggested in Ref. [23], an estimate of the HQSF from the simulation of the non-linear pilot/vehicle system may be obtained from

$$\text{HQSF}(\omega_i) = \frac{\int_0^T u_m(t)\exp(-j\omega t)|_{\omega=\omega_i}\,\mathrm{d}t}{\int_0^T c(t)\exp(-j\omega t)|_{\omega=\omega_i}\,\mathrm{d}t}\left|\frac{1}{K_e}\right|$$

with u_m denoting the proprioceptive feedback signal in the SPM and $c(t)$ denoting the time evolution of the input to the SPM.

2.5 University Roma Tre

The UROMA3 comprehensive helicopter simulation model, suitable for RPC analysis, is obtained by coupling flexible fuselage dynamics, main rotor aeroelasticity, control chain dynamics and pilot behavioural dynamics. The main rotor model interacts both with fuselage dynamics (through hub loads and motion) and with the control-chain servoelastic model which yields the rotor blade pitch controls derived from pilot's commands. The pilot behavioural model receives the vehicle motion as input and supplies the control lever displacement. Each component of the helicopter model is developed with a suitable number of degrees of freedom, representing the optimal trade-off between accuracy and computational efficiency.

2.5.1 Main rotor aeroelastic model

A non-linear, bending-torsion, beam-like model that is valid for straight, slender, homogeneous, isotropic, non-uniform, twisted blades undergoing moderate displacements is applied to represent the structural dynamics of the main rotor [24, 25]. The resulting structural operator consists of a set of coupled, non-linear, differential equations governing the bending of the elastic axis (lead-lag and flap deflections) and the rotation of the cross sections (blade torsion).

Blade aerodynamic loads may be simulated either by a sectional model with Pitt-Peters dynamic-inflow corrections to account for the three-dimensional effects from trailing vortices, or through a Boundary Element Method (BEM) solver for free-wake, potential flows. The BEM computational tool considered is based on a boundary integral equation formulation suited for the prediction of rotor aerodynamics, applicable to a wide range of flight configurations, with inclusion of those characterized by complex blade-vortex interactions [26, 25].

The Galerkin approach is applied for the spatial integration of the resulting aeroelastic integro-differential formulation, while time responses are computed through a time-marching, Newmark-β numerical scheme. Once the rotor aeroelastic response is computed, the corresponding forces and moments at the hub attachment point are evaluated through a combination of aerodynamic and inertial blade loads.

When linear time invariant (LTI) modelling is required for an eigenvalue stability analysis, the state-space representation of the rotor aeroelastic behaviour is identified through the approach presented in Ref. [27]. This approach requires the prediction of a set of harmonic

perturbation responses by a time-marching aeroelastic solver. The accuracy of this solver characterizes that of the identified finite-state operator. It relates hub motion dofs and blade pitch controls to the corresponding loads transmitted to the fuselage by a constant-coefficient, linear, differential form, with the by-product of introducing some additional states deriving from wake vorticity and blade dynamics (indeed, blade dofs do not appear explicitly in this model, but equivalent internal dynamics simulates their influence).

2.5.2 Fuselage model

In RPC occurrence, a crucial role is played by fuselage dynamics. In particular, as demonstrated by past investigations, pilot seat vibrations due to fuselage elastic dynamics are of fundamental importance in PAO phenomena [28, 29]. The fuselage model considered here is obtained by combining the rigid-body equations with those governing the elastic deformations.

The rigid-body equations derive from the standard six dofs model coupled with the kinematics of the Euler angles for the definition of vehicle orientation, (linearized about an arbitrary steady flight condition, for LTI analyses). The main forcing terms of these equations are the loads at the main rotor hub, but contributions from the tail rotor and fuselage aerodynamics are taken into account, as well.

Fuselage elastic dynamics are expressed through a linear modal approach with mass, damping and stiffness matrices identified through a FEM analysis dedicated to the evaluation of free-vibration modes of the unconstrained structure. It is forced by the projection of the main rotor and tail rotor loads onto the modal shapes derived from the eigenvectors given by the FEM analysis. Indeed, this is a convenient approach, in that the resulting elastic modes are such that rigid-body motion equations and elastic dynamics equations are coupled only through the forcing terms [29].

2.5.3 Pilot and control-chain models

For the frequency range of interest in PAO phenomena (that are those of concern in aeroservoelastic RPC), the pilot acts as an inadvertent link between the seat motion and the controls, practically acting like a mechanical impedance.

Passive (involuntary behaviour) models of helicopter pilots are introduced in terms of transfer functions between the seat acceleration (input), and the vertical acceleration of the pilot's hand (output). These vary as function of pilot mass, pilot workload, commands setting. One of the first attempts to model passive pilot behaviour was conducted by Mayo, who identified ectomorphic (lighter) and mesomorphic (heavier) pilot models that are particularly suited for vertical bouncing analysis, in a dedicated experimental campaign [30].

Pilot's commands are transmitted to rotor blades through the control chain. This transmission is modelled by second-order differential forms relating stick rotation (and pedals) to main rotor (and tail rotor) blade pitch controls.

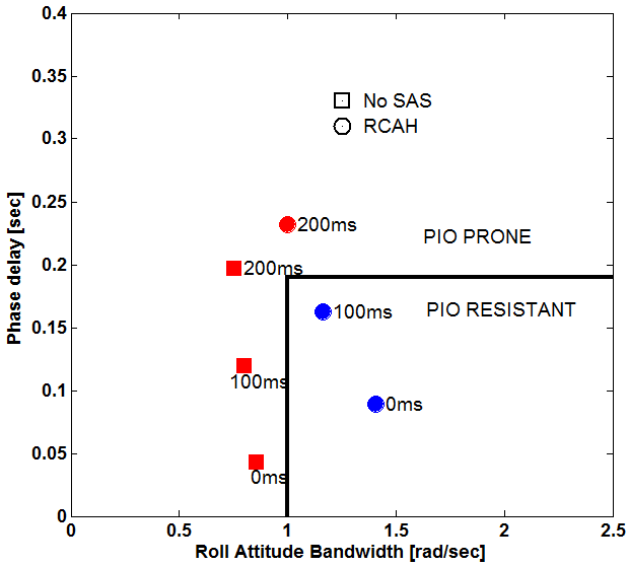


Figure 7. Bandwidth-phase delay for roll axis at hover.

3. NUMERICAL RESULTS

This Section presents some selected results relating to aeroservoelastic PAO analyses of small-size and medium-size helicopters carried out by ARISTOTEL's partners. These are part of the numerical investigations aiming at the final project goal to provide design guidelines and methodologies for the prevention of adverse RPC/PAO in the next generation of helicopters.

3.1 ONERA

First, the medium-size IAR330 Puma helicopter RPC behaviour is examined. Figure 7 presents the bandwidth-phase delay in the roll axis at hover, for both the helicopter without a stability augmentation system (SAS), and the augmented RCAH helicopter. To create Cat I PIO proneness, time delays were introduced to the flight control system. It can be seen that the unaugmented IAR330 Puma is PIO prone, whilst the augmented helicopter is PIO resistant until an additional time delay of between 100ms and 200ms is introduced into the flight control system.

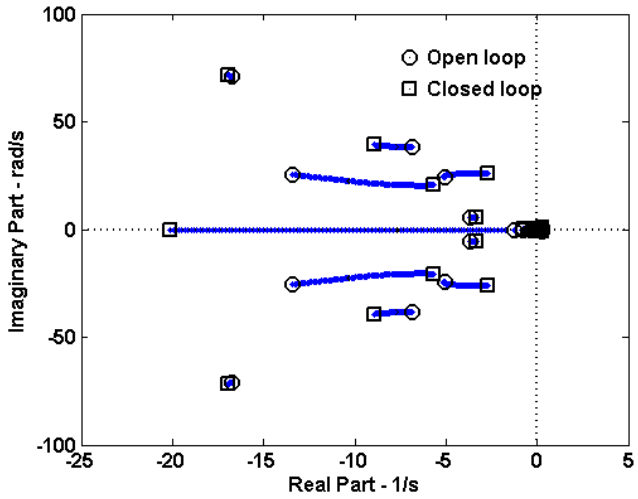


Figure 8. Root locus of bare IAR330 Puma with collective control feedback in hover flight.

The above results are found to be identical to the rigid-body models. The explanation is that the rotor elastic modes have no influence on the determination of the parameters that are used in this PIO criterion. The bandwidth used in the criterion is the lesser of the gain and phase margin bandwidths. The gain margin bandwidth is defined as the frequency for 6dB of gain margin while the phase margin bandwidth is the frequency at which the phase margin is 45 deg [9]. Figure 8 displays the dynamic characteristics of the bare airframe IAR330 Puma helicopter at the hover flight condition, with the passive pilot closing the loop through the collective control. As shown on the Figure, the pilots poles at $-5.08 \pm 24.44i$ move closer to the stability boundary to $-2.68 \pm 25.96i$ as the pilot closes the loop. The flap mode also moves closer to the stability boundary from $-13.39 \pm 25.31i$ to $-5.70 \pm 20.53i$.

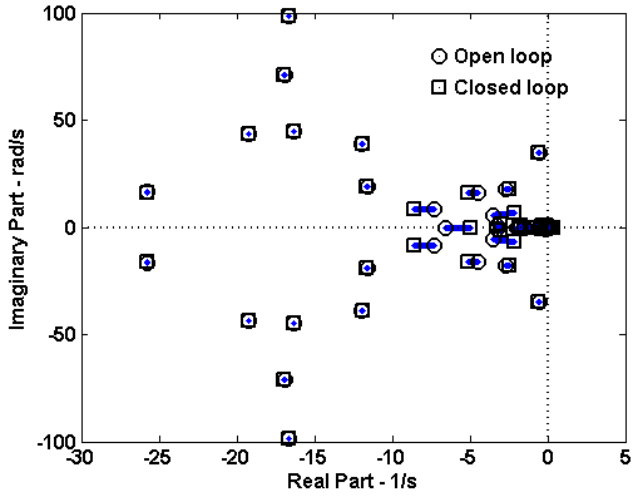


Figure 9. Root locus of coupled active/passive pilot-IAR330 Puma in forward flight.

Zooming in on the flight mechanics modes indicates that the most noticeable migration relates to the roll subsidence at -0.34 and the pilots poles at the origin which degenerate into a pair of complex conjugate $-0.08 \pm 0.20i$ and a real poles at -20.11. The unstable dutch roll mode at $0.096 \pm 0.54i$ and phugoid mode at $0.29 \pm 0.59i$ remain unchanged. The flight control law of the RCAH IAR330 Puma provides better rigid body handling qualities than the bare IAR330 Puma configuration, whilst leaving the rotor elastic modes unchanged. From the analysis of the dynamic characteristics of the RCAH IAR330 Puma helicopter in hovering flight, it can be seen that, unlike the bare IAR330 Puma, the pilots poles and the flap mode remain unchanged as the pilot closes the loop. Figure 9 displays the dynamic characteristics of the RCAH IAR330 Puma helicopter at 80 kt forward flight, with the passive pilot closing the loop through the lateral cyclic control and the active pilot performing a PT roll-step manoeuvre.

As the passive pilot closes the loop, the progressive lag mode remains practically unchanged while the regressive lag mode at $-2.69 \pm 17.83i$ moves slightly closer to the stability boundary to $-2.42 \pm 18.00i$. A zoomed-in plot of the flight mechanics modes (see Fig. 10) shows the modes introduced by the PT guidance law. The destabilizing effect of the passive pilot is illustrated by the degeneration of the outer-loop guidance complex pole $-0.10 \pm 0.31i$ into two unstable real poles 0.20 and

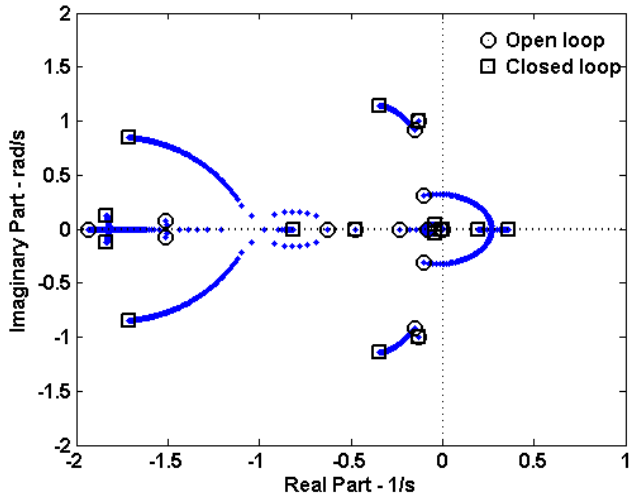


Figure 10. Flight mechanics root locus of coupled active/passive pilot-IAR330 Puma in forward flight.

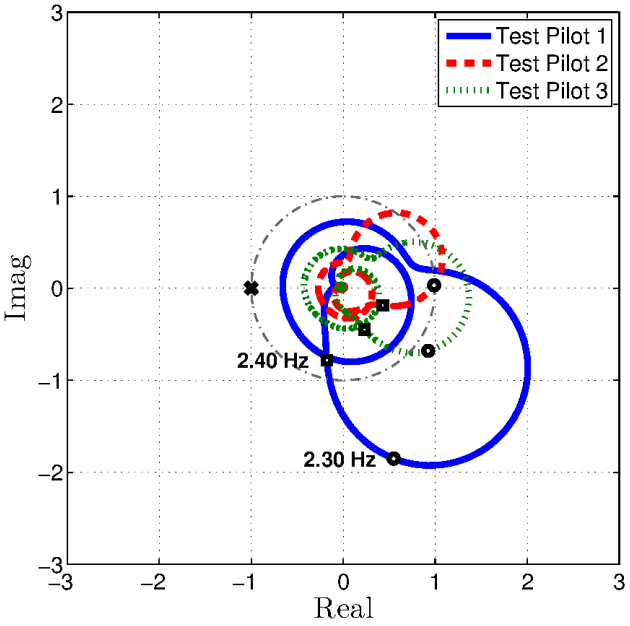


Figure 11. Nyquist plots of the LTF for the three test pilots in feedback loop with the Bo-105 at 80 kts, with $G_y = 2.5$ and $\tau y = 0$ ms. (◯): 2.30 Hz; (□): 2.40 Hz.

0.36.

3.2 Politecnico di Milano

The results of the lateral oscillations in forward flight, on the linearized Bo105 model, are shown in Fig. 11 and Fig. 12. The configuration in Fig. 11 is characterized by a larger lateral gearing ratio (G_y = 2.5 times the nominal value) and nil time delay. The increase in the gain alone is not sufficient to destabilise any of the closed loop systems, as shown by the Nyquist curves. However, test pilot 1 appears to be more prone to instability since the corresponding LTF is characterized by a larger amplitude and a smaller phase margin, as a consequence of the higher static gain and lower natural frequency of the pilot's biodynamic pole [10]. The Next configuration (Fig. 12) presents a 100 ms time delay, with the same lateral gearing ratio as the previous case. The time delay produces a clockwise rotation of the Nyquist curves, that results in a significant reduction of the phase margin, driving test pilot 1 towards a PAO instability. The Nyquist plot for test pilot 1 shows that the control system time delay is the key factor that generates the pilot response in phase opposition to the helicopter dynamics. A PAO instability at 2.34 Hz is triggered, as a result of an aeromechanical instability (air resonance) created by the lightly damped main rotor regressive lead-lag mode, coupled with the pilot 1 biodynamics/lateral stick dynamics.

Results from time marching simulations, obtained in MB-Dyn, are shown in Fig. 13. The tracking of the desired trajectory is obtained using a simple model of the pilot's intentional behaviour based on the crossover model [13], with a feedforward contribution [14]. The collective pitch requested to the control system,

$$\vartheta = \vartheta_{AP} + \vartheta_{ff} + \vartheta_{PP}$$

is thus made of three contributions: a voluntary part, ϑ_{AP}, which includes some form of the feedforward $\vartheta_{ff} = H^{-1}_{z\vartheta}(s) \cdot z_0$, where $H^{-1}_{z\vartheta}(s)$ is the inverse of the vehicle transfer function, low-pass filtered to become strictly proper, and an involuntary part, ϑ_{PP}, consisting of the control inceptor rotation caused by the biodynamic feedthrough (BDFT), scaled by the gearing ratio,

$$\vartheta_{PP} = G \cdot H_{BDFT}(s) \cdot \ddot{z}$$

The gearing ratio G that drives the system to the verge of stability (more than twice the nominal value) is consistent with the value obtained modeling the BDFT using experimental transfer functions, thus providing a further indirect confirmation of the suitability of the biomechanical model of the pilot's arm for the purpose of estimating the stability of the coupled system.

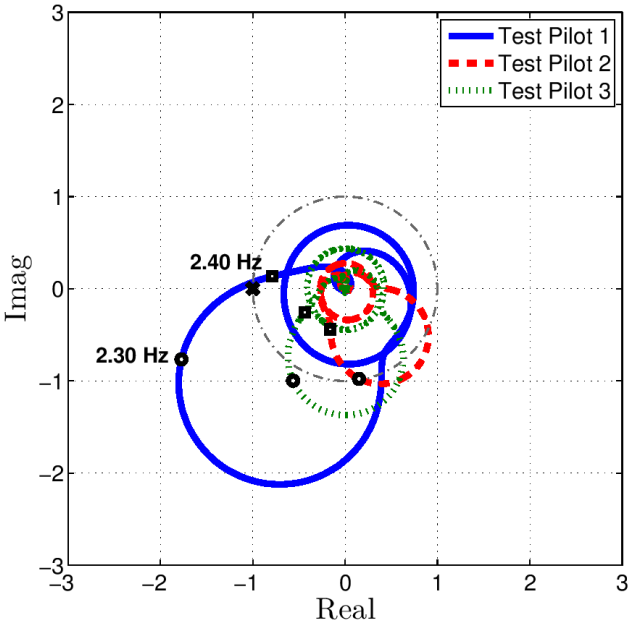


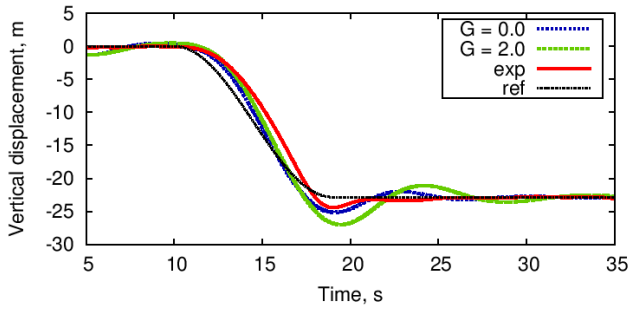
Figure 12. Nyquist plots of the LTF for the three test pilots in feedback loop with the Bo-105 at 80 kts, with $G_y = 2.5$ and $\tau y = 100$ ms. (◯): 2.30 Hz; (□): 2.40 Hz.

3.3 University of Liverpool

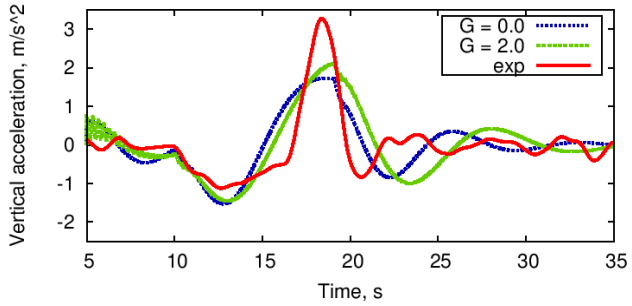
The elastic blade models for the Bo105 and IAR330 Puma created in FLIGHTLAB have been compared to those obtained from MASST as a means of an initial validation of the model. This comparison has taken a number of forms:

- mode frequency comparison at 100% RPM;
- mode shape comparison;
- fan plot comparison.

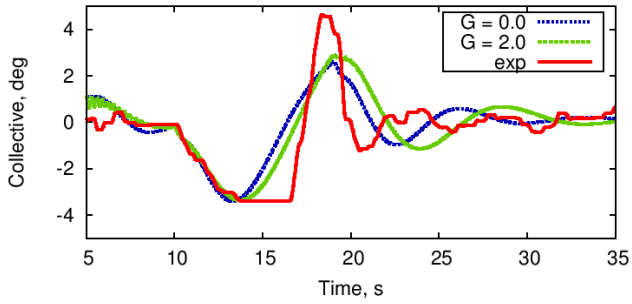
The mode frequencies (first 7 modes at 100% RPM) obtained from both tools for both rotorcraft models are plotted in Fig. 14. These show that the frequencies of the first seven modes from both of the elastic rotor models are in good agreement, within 2% of each other. Fig. 15 presents fan plot prediction comparisons for IAR330 Puma and Bo105 main rotors. This figure again shows good consistency between the FLIGHTLAB and MASST results, especially for the first lag, flap and second flap modes. For the third flap, second lag and first torsion modes of the Puma rotor, good agreement has been achieved below 80% RPM but above



(a) Vertical position at the pilot seat



(b) Vertical acceleration at the pilot seat

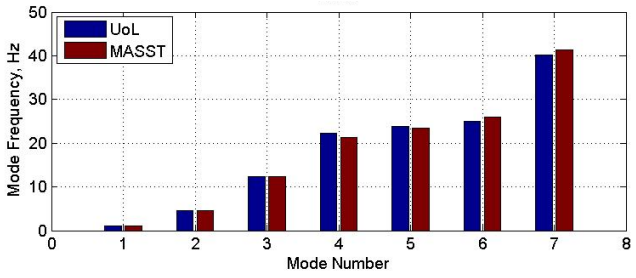


(c) Collective control rotation

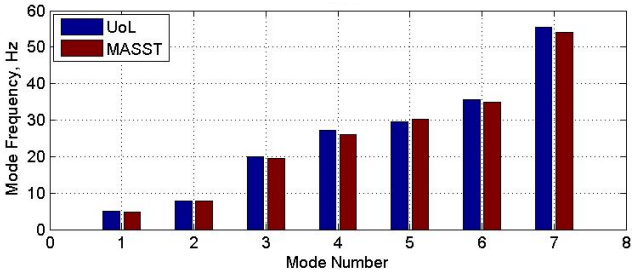
Figure 13. Vertical maneuver performed on the multibody model of the IAR330 Puma. Results compared with the experimental tests performed at the flight simulator of UoL.

this value, the results show a slight difference in frequency of up to 8%. This may be due to the different algorithms within FLIGHTLAB and MASST used to perform the calculations on the isolated rotor model. For the Bo105 rotor, these modes still have good agreement with each other.

Four mode nodes were selected to model the elastic fuselage (main rotor, tail rotor, pilot, and co-pilot). The non-linear aeroelastic models are built in FLIGHTLAB by combining the mode shapes generated from the iso-

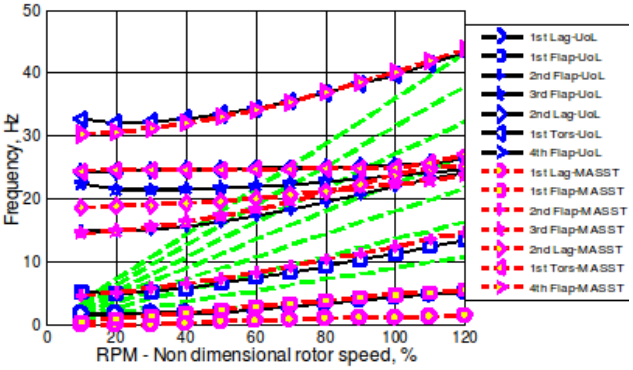


(a) IAR330 Puma

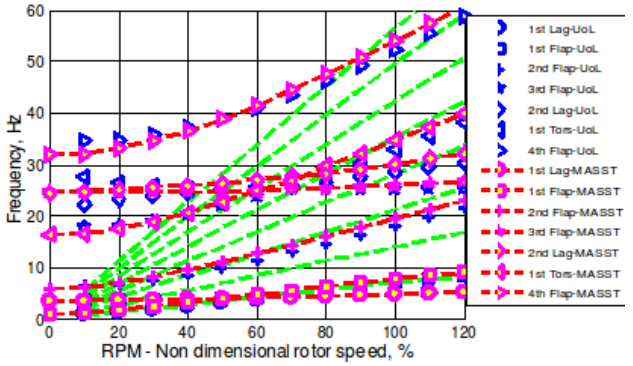


(b) Bo105

Figure 14. Mode frequency comparison between MASST and FLIGHTLAB.



(a) Puma-IAR330



(b) Bo105

Figure 15. Calculated fan diagram.

lated elastic rotors, noted above and the elastic fuselage. The fidelity of these two models were first validated by comparing their eigenvalues with those of rigid-body versions and the values in Ref. [17] as well (denoted HFD in subsequent Figures). The results with six degree-of-freedom (6DOF) are shown in Figs. 16 and 17. For the elastic IAR330 Puma model, Fig. 16 shows that the eigenvalues can be significantly affected by the additional elastic contributions from the main rotor and fuselage. For the elastic Bo105 model, the eigenvalues of three sources have reached good agreement. Moreover, Fig. 17 shows that the elastic results are closer to those presented in HFD For instance, the dutch mode of the elastic model fits better with those of HFD and the distribution of the phugoid mode appears more consistent. Furthermore, the 74th-order results also compare well with those from MASST.

The fidelity of the developed Bo105 model is further verified by comparing the responses with flight test data provided by the German Aerospace Centre (DLR). The results of the time-response verification are assessed by driving the model with a doublet input, as shown in Fig. 18 for the longitudinal cyclic command (responses to lateral cyclic, collective and pedal commands are available, but are not presented for conciseness). As these results demonstrate, the developed elastic model generally fit the flight test data well for the on-axis responses for all four control channels (e.g., the pitch response from the longitudinal input and the roll response from the lateral input). The agreement with the flight test off-axis responses is not as good as the on-axis responses. These findings resemble those from the rigid-body responses compared with the flight test data.

3.4 STRAERO

3.4.1 Rotorcraft aeroelastic analysis

The solution process described in Section 2.4.1 was monitored in terms of blade tip displacement and blade load. Consider the helicopter IAR330 Puma, flapping displacement and the total normal load on the main rotor have been compared with the experimental data for validation purposes.

For the numerical simulation, the type of solution was

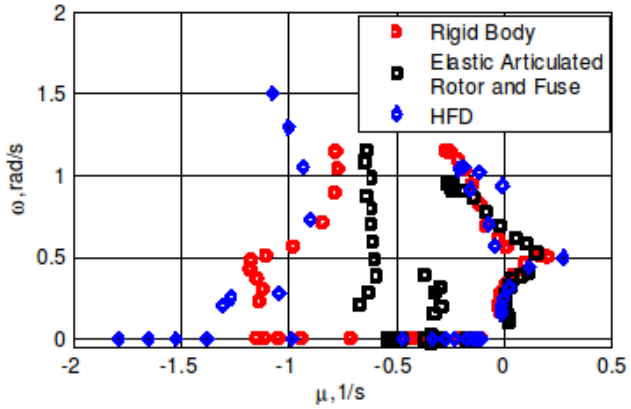


Figure 16. Eigenvalues from IAR330 Puma simulation models.

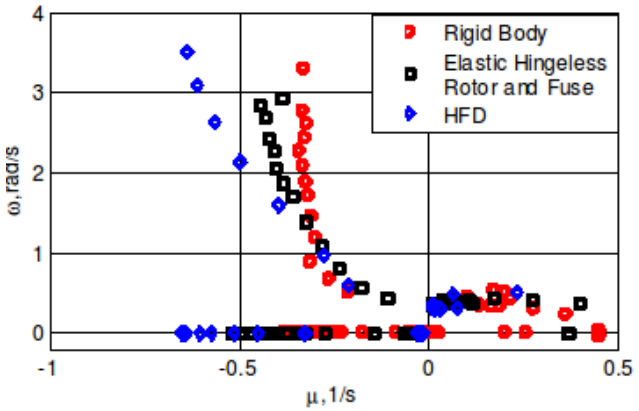


Figure 17. Eigenvalues from Bo105 simulation models.

chosen as transient for both the structural solver and the aerodynamic one, with a time step corresponding to a blade rotation of 3.17 deg. For all variables involved, the convergence criteria and the relaxation values were set equal to 0.001 and 0.75, respectively [19].

The helicopter was filmed with a high speed camera in hover flight and a 600 mm displacement of blades tip was measured using image processing techniques. Comparing it to the 610 mm displacement computed in our solution (see Figs. 19 and 20) we may conclude that the numerical solution is in good agreement with the flight tests. Also, the computed rotorcraft load of 72904 N is in good agreement with the helicopters weight.

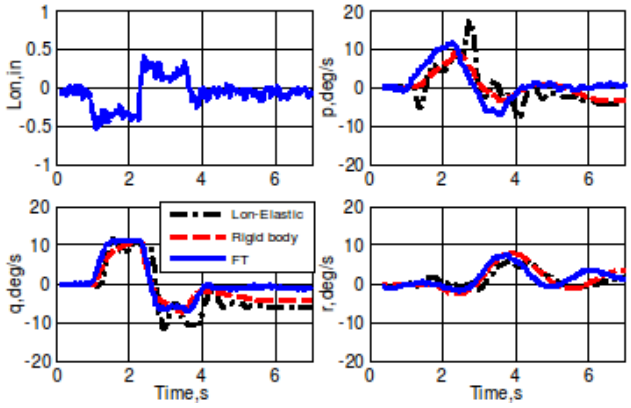


Figure 18. Response of the elastic BO105 model to longitudinal cyclic doublet inputs compared with flight test data.

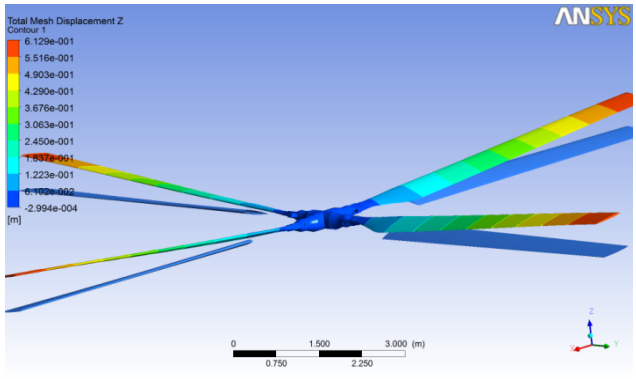


Figure 19. Simulated coning of the main rotor in hover.

3.4.2 RPC susceptibility analysis

The helicopter IAR330 Puma has been considered in an 80 kts speed forward flight condition at sea level. The behaviour of the rotorcraft coupled with the pilot in the loop is examined for the 'pitch up' manoeuvre following the analysis method of Section 2.4.2, with the ratio of Fourier transformation in the definition of HQSF evaluated for the upper limit of $T = 10$ sec. The bounds on HQSF and the normalized $\Phi_{u_m u_m}$ define the HQ levels, while PIOR levels defined for linear systems is demonstrated that can be conveniently applied for non-linear systems analysis, as well. This case study on linear and non-linear models (with displacement limits) of RPCs is an example of how to apply a unified theory for handling qualities and PIO to rotorcraft. The corresponding outcomes are presented in Figs. 21 and 22. These have been obtained by a computer program

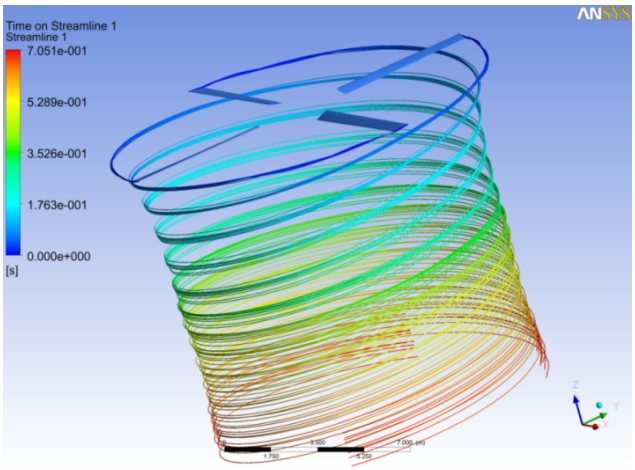


Figure 20. Streamlines released from blades tip.

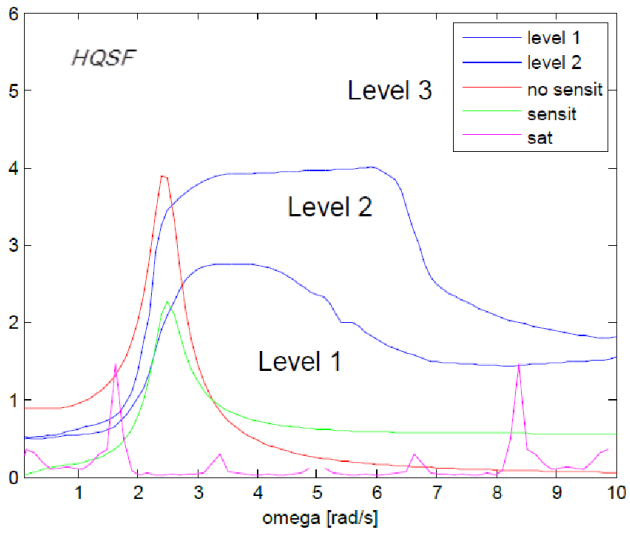


Figure 21. HQSF for flight level configuration with 7 deg longitudinal cyclic displacement limit.

resulting from the implementation of pilot and rotorcraft aeroservoelastic models, that provides the prediction of handling qualities levels and PIO levels.

3.5 University Roma Tre

In the following, a selection of the analyses carried out by UROMA3 on aeroservoelastic PAO/RPC is presented. These concern the RPC/PAO event called vertical bouncing, which is the result of a potentially destructive closed loop consisting of the coupling between main rotor collective pitching and coning, airframe (rigid and elastic) vertical motion and collective lever motion, driven by the pilot feedthrough as inadvertent actuation of the control stick due to vertical oscillation of the seat [30, 29]. Considering the Bo105 helicopter in the hover condition, Figs. 23 and 24 show the show the eigenvalues of the hovering helicopter dynamics, as evaluated using sectional aerodynamics and BEM aerodynamics, respectively, with and without ectomorphic pilot in the loop ('Gain' denotes the gain of the Mayo pilot model applied [30]). The helicopter dynamics predicted by these two models is similar (especially concerning the rigid-body modes, as expected), but appreciable differences appear between the eigenvalues related to the mode dominated by the pilot biodynamics and the eigenvalues related to the first lag collective elastic mode. In particular, the first lag collective elastic mode predicted by application of the sectional aerodynamics formulation is significantly less damped than that obtained from BEM aerodynamics. This occurs regardless of the presence of the pilot in the loop which, in any case, tends to decrease the stability margin of this mode.

Next, non-linear, time-marching responses to perturbations evaluated for the piloted Bo105 are presented in Fig. 25. These concern pilot gains $G = 0.6$ and $G = 0.9$, advance ratio, $\mu = 0.2$, and confirm the outcome of the linear eigenvalue analysis which predicted a very small stability margin for the case with $G = 0.9$. A direct comparison of linear and non-linear dynamic analyses of the piloted Bo105 is presented in Fig. 26, for $G = 0.9$. It demonstrates that, although non-linear terms induce some modification of the response damping, the linear (eigenvalue) analysis yields a reliable estimate of the piloted helicopter dynamics, and hence is a good tool to consider RPC effects in the design process. Finally, Figs. 27 and 28 present helicopter dynamics roots as predicted by different pilot models, each related to a different workload (so-called, relaxed, force and precision tasks in Ref. [31]). Figure 27 concerns the hovering Bo105, whereas Fig. 28 concerns the IAR330 Puma at advance ratio, $\mu = 0.2$. In both cases, the relaxed-task pilot model is the one that more strongly couples with the first airframe mode and is more prone to unstable RPC, while the force-task pilot model yields roots more slowly moving towards instability as the gain increases.

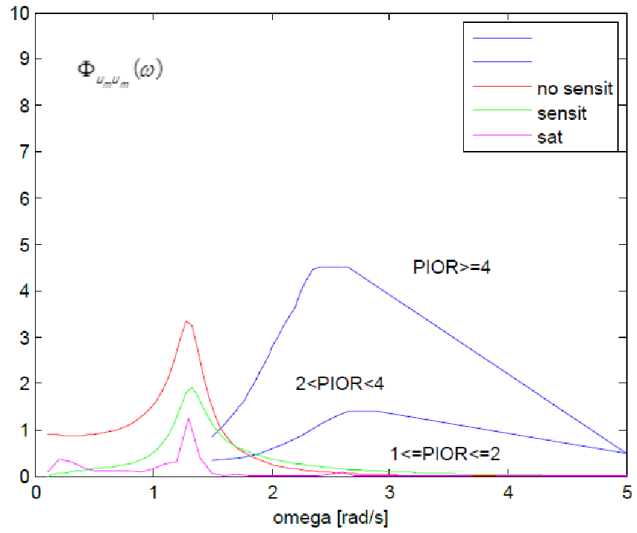


Figure 22. Normalized $\Phi_{u_m u_m}$ for flight level configuration with 7 deg longitudinal cyclic displacement limit.

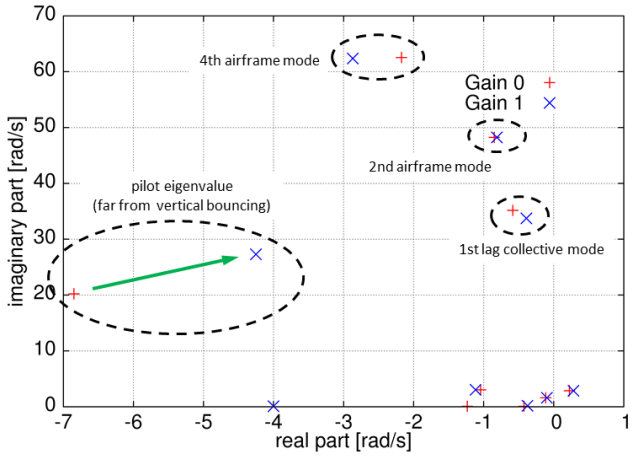


Figure 23. Bo105 dynamics roots, with and without pilot in the loop. Hovering condition, sectional aerodynamics.

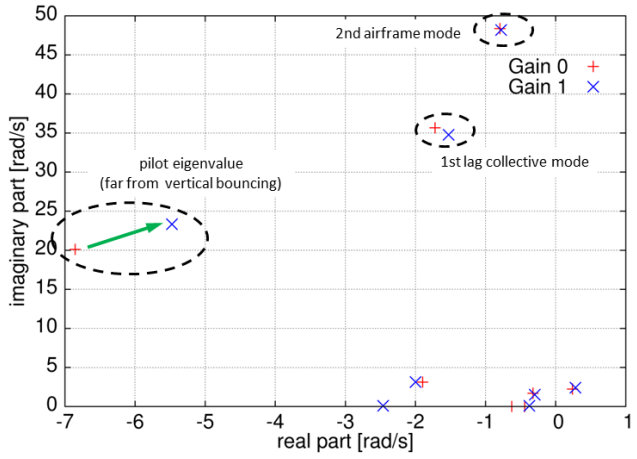


Figure 24. Bo105 dynamics roots, with and without pilot in the loop. Hovering condition, BEM aerodynamics.

4. CONCLUSIONS

In the following, some conclusions derived from the observation of the numerical investigations presented above are given, as related to each partner's activity. These are only partial considerations that will contribute to the definition of design guidelines for prevention of adverse RPC in new helicopter configurations, and that will be further developed before teh conclusion of the project.

ONERA The application of the low bandwidth-phase delay criterion of ADS-33 to the IAR330 Puma helicopter does not capture the effects of the elastic characteristics. By using an eigenvalue analysis method, it was shown that the passive coupling of the pilot biomechanics with the IAR330 Puma helicopter results in lower damped poles in general. Heave coupling in hover flight is characterized by a strong decrease of the damping of the flap mode for the bare IAR330 Puma, while it remains unchanged for the RCAH IAR330 Puma. The coupling of the combined passive pilot and active pilot with the IAR330 Puma model in a roll step manoeuvre leads to the destabilization of the guidance outer loop.

PoliMi PAO events have been predicted with three test pilots flying on the linear aeroservoelastic Bo105 model for specific degradations of the control system parameters. The identification of the biodynamic feedthrough of the pilots indicated that, the vicinity of test pilot 1 lateral biodynamic poles with the lightly damped main rotor first regressive lead-lag mode resulted in a reduction of the phase margin, driving the pilot vehicle system in a lateral PAO instability. The non-linear analyses performed in MBDyn presented the application of a detailed biomechanical model of a helicopter pilot's arm to the bioaeroservoelastic analysis of involuntary adverse rotorcraft-pilot couplings. These results qualitatively resemble analogous experimental data available from the open literature. The

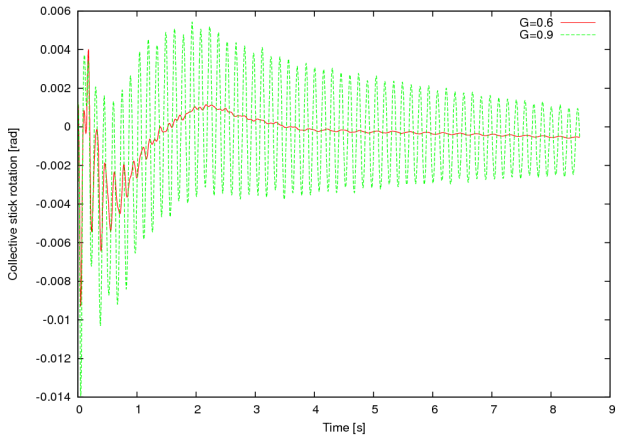


Figure 25. Collective stick rotation response to perturbation predicted by nonlinear Bo105 analysis, for gain $G = 0.6$ and $G = 0.9$. Sectional aerodynamics.

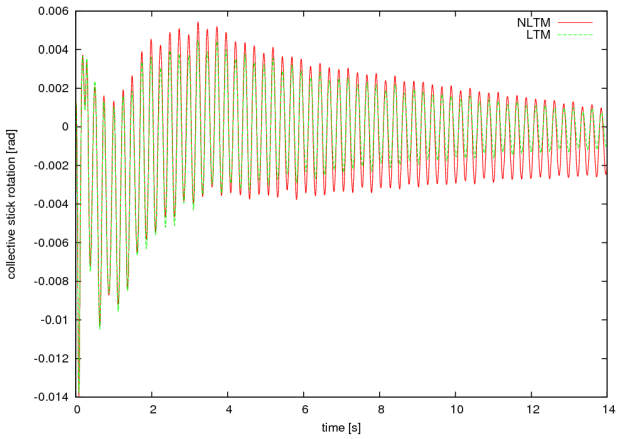


Figure 26. Collective stick rotation response to perturbation predicted by linear and non-linear Bo105 analyses, for gain $G = 0.9$. Sectional aerodynamics.

direct analysis of the coupled system provides the analyst the unique capability to evaluate the sensitivity of complex aeromechanical systems to the biomechanical properties of the pilot.

UoL A series of linear and non-linear aeroelastic models for both Bo105 and IAR330 Puma rotorcraft have been developed at the UoL. Two successful elastic rotor and airframe test campaigns have been conducted on the linear versions of these models. Although the non-linear models have not been used so far due to the limited time availability, the preliminary validation exercise i.e. the comparison with MASST results or with flight test data, indicates that they have reached a good fidelity such that they can be immediately used for future investigations.

STRAERO For the aeroelastic parameters monitored, the rotorcraft model developed yields simulations that appear to be in good agreement with the the physical measurements. Thus, in the future, more complex aeroelastic predictions may be performed without the need of further experimental data. However, the computational effort was massive, and powerful computational platforms will be needed to simulate the aeroelastic response of the rotorcraft in forward flight.Further, a unified theory for handling qualities and PIO to rotorcraft has been presented and applied to linear and non-linear case study helicopter models.

UROMA3 It has been shown that aerodynamic modelling in PAO/RPC predictions affects the eigenvalues of the modes more involved in rotorcraft-pilot coupling. Further, the comparison between linear and non-linear aeroservoelastic piloted helicopter modelling has been presented in terms of predicted responses to perturbations, demonstrating the good capability of the linearized model to capture the PAO/RPC stability behaviour. Finally, three workload pilot models have been applied to Bo105 and IAR330 Puma linearized stability analysis, observing that the so-called relaxed task pilot is the pronest to adverse PAO/RPC.

ACKNOWLEDGEMENTS

The research leading to these results has received funding from the European Union Seventh Framework Programme (FP7/2007-2013) under grant agreement No. 266073.

REFERENCES

[1] M.D. Pavel, M. Jump, B. Dang-Vu, P. Masarati, M. Gennaretti, A. Ionita, L. Zaicek, H. Smaili, G. Quaranta, D. Yilmaz, M. Jones, J. Serafini, J. Malecki,

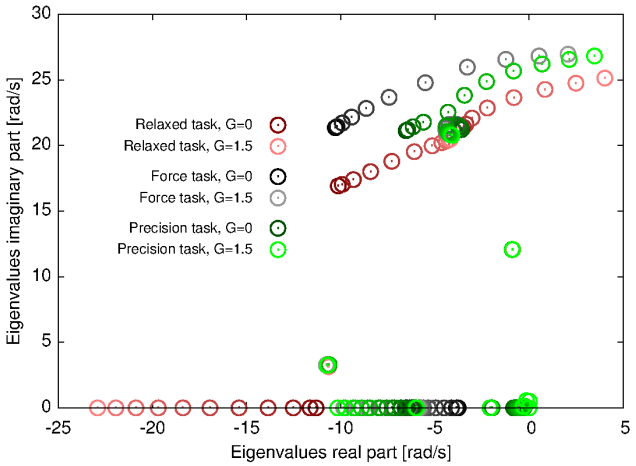


Figure 27. Bo105 dynamics roots for different pilot workloads. Hovering condition, sectional aerodynamics.

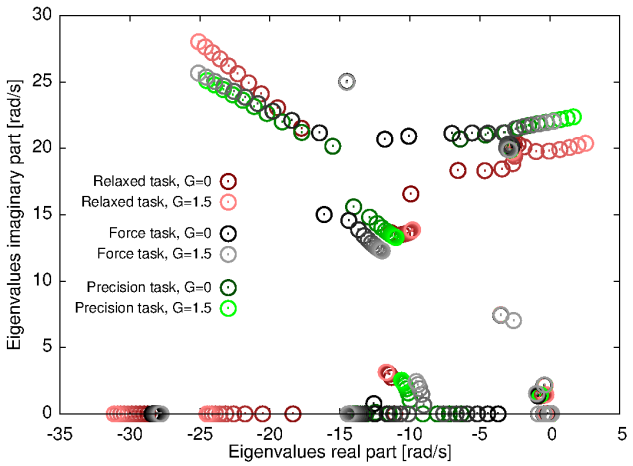


Figure 28. IAR330 Puma dynamics roots for different pilot workloads. Advance ratio $\mu = 0.2$, sectional aerodynamics.

"Rotorcraft Pilot Couplings Past, Present and Future Challenges," *Progress in Aerospace Sciences*, in press. DOI: 10.1016/j.paerosci.2013.04.003.

[2] ARISTOTEL, "Aircraft and Rotorcraft Pilot Couplings - Tools and Techniques for Alleviation and Detection," http://www.aristotel-project.eu/.

[3] M.D. Pavel, D. Yilmaz, "Background, Definition and Classification of A/RPC," Technical Report Deliverable D1.1, EU funded project ARISTOTEL (GA no. 266073), 2010.

[4] O. Dieterich, J. Götz, B. Dang-Vu, H. Haverdings, P. Masarati, M. Pavel, M. Jump, M. Gennaretti, "Adverse Rotorcraft-Pilot Coupling: Recent Research Activities in Europe," 34th European Rotorcraft, Forum, Liverpool, UK, 2008.

[5] B. Benoit, A.M. Dequin, K. Kampa, W. Grünhagen, P.M. Basset, B. Gimonet, "HOST, a General Helicopter Simulation Tool for Germany and France," 56th Annual Forum of the American Helicopter Society, Virginia Beach, VA, 2000.

[6] P. Masarati, V. Muscarello, G. Quaranta, "Linearized Aeroservoelastic Analysis of Rotary-Wing Aircraft," 36th European Rotorcraft Forum, Paris, France, 2010.

[7] M.D. Pavel, D. Yilmaz, B. Dang-Vu, M. Jump, M. Jones, L. Lu, "Adverse Rotorcraft-Pilot Couplings Modelling and Prediction of Rigid Body RPC," 39th European Rotorcraft Forum, Moscow, Russia, 2013.

[8] P. Masarati, et al., "Biodynamic Pilot Modelling for Aeroelastic A/RPC," 39th European Rotorcraft Forum, Moscow, Russia, September 2013.

[9] Anonymous, "Performance specification, handling qualities requirements for military rotorcraft," ADS 33-E-PRF, US Army AMCOM, Redstone, Alabama, 2000.

[10] V. Muscarello, P. Masarati, G. Quaranta, L. Lu, M. Jump, M. Jones, "Investigation of Adverse Aeroelastic Rotorcraft-Pilot Coupling Using Real Time Simulation," 69th Annual Forum of the American Helicopter Society, Paper No. 193, Phoenix, Arizona, May 2013.

[11] V. Muscarello, P. Masarati, G. Quaranta, "Multibody Analysis of Rotorcraft-Pilot Coupling," in P. Eberhard, P. Ziegler (editors), 2nd Joint International Conference on Multibody System Dynamics, Stuttgart, Germany, May 2012.

[12] P. Masarati, G. Quaranta, A. Zanoni, "Dependence of Helicopter Pilots' Biodynamic Feedthrough on Upper Limbs' Muscular Activation Patterns," Proceedings of IMechE Part K: J. Multi-body Dynamics, in press.

[13] D.T. McRuer, H.R. Jex, "A Review of Quasi-Linear Pilot Models," IEEE Transactions on Human Fac-

tors in Electronics, Vol. 8, No. 3, pp. 231-249, 1967.

[14] P. Masarati, G. Quaranta, M. Gennaretti, J. Serafini, "An Investigation of Aeroelastic Rotorcraft - Pilot Interaction," 37th European Rotorcraft Forum, Paper no. 112, Gallarate, Italy, 2011.

[15] Anonymous, *FLIGHTLAB Development Software*, Advanced Rotorcraft Technology Inc., Sunnydale, California.
http://www.flightlab.com/includes/Flightlab.pdf

[16] V. Muscarello, P. Masarati, G. Quaranta, L. Lu, M. Jump, M. Jones, "Investigation of Adverse Aeroelastic Rotorcraft-Pilot Coupling Using Real-Time Simulation," 69th Annual Forum of the American Helicopter Society, Phoenix, Arizona, May 2013.

[17] G.D. Padfield, *Helicopter Flight Dynamics*, 2nd ed., Blackwell Science, Oxford, 2007.

[18] I. Fuiorea, L. Flore, R. Marin, D. Gabor, "A FEM Composite Blade Model Calibration," Efficiency and Innovation through Numerical Simulation ANSYS & Flowmaster Conference, Sinaia, Romania, 2011.

[19] M. Mihaila-Andres, I. Fuiorea, "Aeroelastic Analysis of Rotorcraft Using Ansys," International Conference on Military Technologies, Brno University of Defence, Part II, 2013.

[20] C. Farhat, M. Lesoinne, "Fast Staggered Algorithm for the Solution of Three-Dimensional Nonlinear Aeroelastic Problems," AGARD SMP Meeting, Denmark, 1997.

[21] R.A. Hess, "A Unified Theory for Aircraft Handling Qualities and Adverse Aircraft Pilot Coupling," 35th AIAA Aerospace Sciences Meeting and Exhibit, AIAA-Paper 97-0389, 1997.

[22] A. Ionita, M. Mihaila, I. Fuiorea, L. Lu, M. Jump, M. Jones, B. Dang-Vu, V. Muscarello, P. Masarati, G. Quaranta, M. Gennaretti, J. Serafini, M. Molica Colella, L. Zaichik, H. Smaili, "Aircraft and Rotorcraft modelling for aero-servo-elastic A/RPC," Technical Report Deliverable D3.4, EU funded project ARISTOTEL (GA no. 266073), 2012.

[23] Y. Zeyda, R.A. Hess, W. Siwakosit, "Aircraft Handling Qualities and Pilot-Induced Oscillation Tendencies with Actuator Saturation," *Journal of Guidance, Control and Dynamics*, Vol. 22, No. 6, pp. 852-861, 1999.

[24] D.H. Hodges, E.H. Dowell, "Nonlinear equation for the elastic bending and torsion of twisted nonuniform rotor blades," NASA TN D-7818, 1974.

[25] M. Gennaretti, M. Molica Colella, G. Bernardini, "Prediction of Tiltrotor Vibratory Loads with Inclusion of Wing-Proprotor Aerodynamic Interaction," *J. of Aircraft*, Vol. 47, No. 1, pp. 71-79, 2010.

[26] M. Gennaretti, G. Bernardini, "Novel Boundary Integral Formulation for Blade-Vortex Interaction Aerodynamics of Helicopter Rotors," *AIAA Journal*, Vol. 45, No. 6, pp. 1169-1176, 2007.

[27] J. Serafini, M. Molica Colella, M. Gennaretti, "A Finite-State Aeroelastic Model Rotorcraft Pilot - Assisted - Oscillations Analysis," 38th European Rotorcraft Forum, Amsterdam, The Netherlands, 2012.

[28] M.D. Pavel, J. Malecki, B. Dang-Vu, P. Masarati, M. Gennaretti, M. Jump, M. Jones, H. Smaili, A. Ionita, L. Zaicek, "Present and Future Trends in Rotorcraft Pilot Couplings (RPCs)-A Retrospective Survey of Recent Research Activities within the european project aristotel," 37th European Rotorcraft, Gallarate, Italy, 2011.

[29] J. Serafini, M. Gennaretti, P. Masarati, G. Quaranta, O. Dieterich, "Aeroelastic and Biodynamic Modelling for Stability Analysis of Rotorcraft-Pilot Coupling Phenomena," 34th European Rotorcraft Forum, Liverpool, UK, 2008.

[30] J. Mayo, "The Involuntary Participation of a Human Pilot in a Helicopter Collective Control Loop," 15th European Rotorcraft Forum, Amsterdam, The Netherlands, 1989.

[31] J. Venrooij, M.D. Pavel, M. Mulder, F.C.T. van der Helm, H.H. Bulthoff, "A Practical Biodynamic Feedthrough Model for Helicopters," 38th European Rotorcraft Forum, Amsterdam, Paper no. 096, The Netherlands, 2012.

COPYRIGHT STATEMENT

The authors confirm that they, and/or their company or organization, hold copyright on all of the original material included in this paper. The authors also confirm that they have obtained permission, from the copyright holder of any third party material included in this paper, to publish it as part of their paper. The authors confirm that they give permission, or have obtained permission from the copyright holder of this paper, for the publication and distribution of this paper as part of the ERF2013 proceedings or as individual offprints from the proceedings and for inclusion in a freely accessible web-based repository.